Geometric characteristics of dynamic correlations for combinatorial regulation in gene expression noise

Jiajun Zhang, Zhanjiang Yuan, and Tianshou Zhou
School of Mathematical and Computational Sciences, Sun Yet-Sen University, Guangzhou 510275, People's Republic of China
(Received 16 April 2009; revised manuscript received 28 May 2009; published 7 August 2009)

Knowing which mode of combinatorial regulation (typically, AND or OR logic operation) that a gene employs is important for determining its function in regulatory networks. Here, we introduce a dynamic cross-correlation function between the output of a gene and its upstream regulator concentrations for signatures of combinatorial regulation in gene expression noise. We find that such a correlation function with respect to the correlation time near the peak close to the point of the zero correlation time is always upward convex in the case of AND logic whereas is always downward convex in the case of OR logic, whichever sources of noise (intrinsic or extrinsic or both). In turn, this fact implies a means for inferring regulatory synergies from available experimental data. The extensions and applications are discussed.

DOI: 10.1103/PhysRevE.80.021905 PACS number(s): 87.18.−h, 05.45.Tp, 87.16.Yc

I. INTRODUCTION

Cells live in a complex environment and continuously have to make decisions for different signals that they sense. A challenge in systems biology is to understand how signals are integrated. As the central information-processing units of living cells, transcription regulatory networks allow them to integrate different signals and generate specific responses of genes. The elementary computations are performed at the *cis*-regulatory regions of the genes. The transcription rate of each gene (the output) is a function of the active concentrations of each of the input transcription factors (TFs) [1]. Such a quantitative mapping between the regulator concentrations and the output of the regulated gene is known as the *cis*-regulatory input function (CRIF), which can be modeled by Boolean logics [2,3] in analogy with Boolean calculations that basic electronic devices perform [4]. For example, two activators regulate a gene with AND or OR logic operation (refer to Fig. 1). In fact, AND and OR logic gates are the most frequently accounted instances in the biological literature, surely due to their simplicity and widespread representation in many regulatory processes. For example, the variants of the *lac* promoter display AND and OR behaviors by introducing point mutations [5]. Other examples include that *Pu* variants with stronger binding sequences for specific RNAP make the regulatory module XylR/m-xylene/Pu a robust AND gate [6]; the gene FliLMnoPQR, which makes up the flagella motor, is combinatorially regulated by activator FlhDC and activator FliA with OR logic gate [7]. The notion of logic operations can also be generalized by introducing a continuous function that encodes the dependence of the rate of transcription on the concentrations of inputs [1]. Knowing which mode of combinatorial regulation that a gene employs is important for determining its function in regulatory networks. For example, the *cis*-regulatory module drives cellular patterns differently depending on how the gene integrates intracellular and extracellular signals at its regulatory region by endogenous and exogenous transcription factors [8,9].

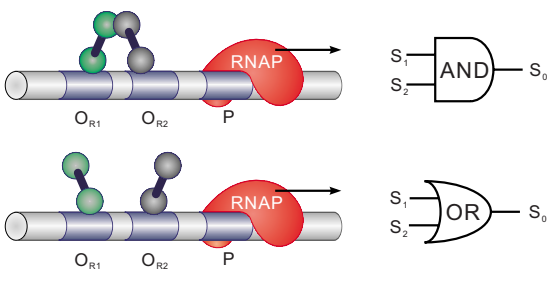

FIG. 1. (Color online) Schematic illustration of *cis*-regulatory constructs. The regulatory functions are realized through the regulated recruitment of transcription factors and RNA polymerase (RNAP).

Experiments performed on single cells have revealed that because TFs are often present in low copy numbers, stochastic fluctuations or noise in the concentrations of these molecules can have significant influences on gene regulation [10–13]. The traditional fluctuation-dissipation relation derived by the linear noise approach [14] based on the master equation gives the information only about the second-order moments. Recently, a modified fluctuation-dissipation relation was derived by Warmflash and Dinner [15], which relates some third-order moments evaluated at the system steady state to the derivatives of a CRIF. Such a *static cross correlation* provides the information only about how three time series are correlated at the zero correlation time. From viewpoints of gene regulation, however, the binding of TFs to the DNA is context dependent, active in some genetic states but not in others. In particular, stochastic fluctuations or "noise" in gene expression propagate from active inputs to the outputs of regulated genes during signal integration. Thus, *dynamic cross correlations* [16,17] would provide a noninvasive means to probe modes of combinatorial regulation in gene expression noise. The purpose of this paper is to demonstrate its potentials in detecting signatures of combinatorial interaction. Regarding the study of combinatorial regulation, there are other works [18–22]. Usually, these papers used some real time-course microarray data to test their algorithms and identify some synergistic TFs, e.g., Chen *et al.* [19], used a kinetic model to select the combinatorial control of multiple TFs: selection of thermodynamic models for combinatorial control of multiple TFs in early differentiation of embryonic stem cell.

Thanks to the idea of two recent works [15,17], we introduce *dynamic three-point cross correlation* that relates the output of a gene to its inputs (more precisely, the dynamic cross correlation is defined as the convolution of the output and input signals). Such a correlation function has the following advantages. (1) It can be used to deal with the simultaneous presence of intrinsic and extrinsic noise. (2) It is the generalization of the fluctuation-based relations derived by Warmflash and Dinner [15] (in fact, the static three-point cross correlation derived by Warmflash and Dinner is a particular dynamic three-point cross correlation at the zero correlation time) and can be used to more efficiently identify the modes of combinatorial gene regulation from experimentally measured time series of the concentrations of the species composing the regulatory process. (3) It can even be used to probe the activity states of regulatory links.

For clarity and simplicity, in this paper we consider only the case that two input transcription factors regulate the expression of a gene (whose level is taken as the output) with AND or OR logic operations. Interestingly, we find that the cross-correlation curve with respect to the correlation time near the peak is upward convex in the case of AND, whereas downward convex in the case of OR. In particular, we show the different effects of intrinsic and extrinsic noises on the dynamic cross correlations, e.g., the intrinsic noise determines the convexity of the cross-correlation curves, whereas the extrinsic noise generally does not affect the convexity but can shift the location of the correlation curve upwards. According to the convexity of the cross-correlation curve, we can in turn distinguish the AND operation from the OR operation. In addition, we find that there is always a time lag between the extreme point of the cross-correlation function and the zero correlation time, which can be used to determine the direction of interactions among regulators. For this, we give some discussions in the final section.

II. GEOMETRIC CHARACTERISTICS OF CROSS CORRELATIONS IN A REAL GENETIC CIRCUIT

Before presenting our theoretical results, let us examine a real biological example. Consider a genetic circuit based on the phage-λ operon [15,23]. In the construct of this system, the P_{RM} promoter and $O_{\mathrm{R}}2$ binding site are in their natural locations and an additional binding site for the *Escherichia coli lac* activator cyclic AMP receptor protein (CRP) is located upstream; the gene cI activates transcription by binding to $O_{\mathrm{R}}2$ and the output is lacZ. The original construct is an AND logic gate. Similarly, we can also construct an OR logic gate by a few point mutations [5,24].

Denote by $D_i(i=0,1,2)$ as the DNA regulatory sequences of genes, which encode proteins lacZ, CRP, and cI $[S_i(i=0,1,2)]$, respectively. Also, denote by $M_i(i=0,1,2)$ as the mRNA molecules and P as the RNA polymerase. The genes can randomly produce and degradate the proteins with the same rate, but the production or degradation depends on the state of the operator $D_i(i=0,1,2)$. The *cis*-regulatory constructs are schematically shown in Fig. 1, where TFs S_1 and S_2 are taken as inputs, whereas S_0 as the output. Assume that TFs S_1 and S_2 can combinatorially bind to the operator D_0 in the form of monomer. In the case of AND gate, the output gene can be expressed only when both input TFs S_1 and S_2 bind to the operator D_0 cooperatively. In the case of OR gate, however, the output gene can be transcribed when one or both of the input TFs bind to the target operator. The parameters listed in Table I for the OR logic gate are from Ref. [15], which are used to simulate the idealized logic gates. The parameters for the AND logic gate are the same as for the OR logic gate except that the transcription rates are set to zero when only one input TF binds to D_0.

TABLE I. Reactions and parameter values for simulations of the logic gate in the idealized system (used in the presence of intrinsic noise only). The reactions include the TF binding to the DNA promoter, transcription, translation, and degradation of mRNAs and proteins.

Descriptions	Reactions	k_f	k_b
Transcription	$\varnothing \rightarrow M_1$	5	
Translation	$M_1 \rightarrow M_1 + S_1$	10	
mRNA degradation	$M_1 \rightarrow \varnothing$	1	
Protein degradation	$S_1 \rightarrow \varnothing$	1	
Transcription	$\varnothing \rightarrow M_2$	5	
Translation	$M_2 \rightarrow M_2 + S_2$	10	
mRNA degradation	$M_2 \rightarrow \varnothing$	1	
Protein degradation	$S_2 \rightarrow \varnothing$	1	
RNAP binding to DNA promoter	$D_0 + S_1 \rightleftharpoons D_0S_1$	10	500
RNAP binding to DNA promoter	$D_0 + S_2 \rightleftharpoons D_0S_2$	10	500
S_2 binding to D_0S_1 complex	$D_0S_1 + S_2 \rightleftharpoons D_0S_1S_2$	10	250
S_1 binding to D_0S_2 complex	$D_0S_2 + S_1 \rightleftharpoons D_0S_1S_2$	10	250
Transcription	$D_0 \rightarrow D_0 + M_0$	0	
Transcription	$D_0S_1 \rightarrow D_0S_1 + M_0$	20	
Transcription	$D_0S_2 \rightarrow D_0S_2 + M_0$	20	
Transcription	$D_0S_1S_2 \rightarrow D_0S_1S_2 + M_0$	20	
Translation	$M_0 \rightarrow M_0 + S_0$	10	
mRNA degradation	$M_0 \rightarrow \varnothing$	1	
Protein degradation	$S_0 \rightarrow \varnothing$	1	

In order to illustrate sources of noise, such as the presence of intrinsic noise only and the simultaneous presence of extrinsic and intrinsic noises, we give the corresponding chemical reactions separately in Tables I and II, which are divided into two categories: reversible (DNA-binding reactions and multimerization) and irreversible (transcription, translation, and degradation). In the idealized logic gate (Table I), we assume that the rate of the DNA state change is fast enough and the fluctuating DNA state has been replaced with the equilibrated state by neglecting the explicit dynamics of DNA state alteration (which is called the adiabatic approximation) [25]. In this strong adiabatic limit, the stochastic fluctuations in three genes involved in logic gates lead to the so-called intrinsic noise. Since the DNA state alters much more slowly in eukaryotes than in prokaryotes, the actual dynamics of the DNA state can be in the weakly adiabatic or nonadiabatic situation, which can be modeled by transitions between "on" and "off" states. In addition, genes in a single cell may be affected by some global fluctuations (i.e., so-

TABLE II. Reactions and parameter values for simulations of the logic gate (used in simultaneous presence of intrinsic and extrinsic noise). The reactions also include the TF and RNA polymerase binding to the DNA promoter, transcription, translation, degradation of mRNAs and proteins, and DNA-binding proteins to recruit RNA polymerase and DNA state.

Descriptions	Reactions	k_f	k_b
RNAP binding to DNA promoter	$D_1+P \rightleftharpoons D_1P$	10	500
Transcription	$D_1P \rightarrow D_1P+M_1$	5	
Translation	$M_1 \rightarrow M_1+S_1$	10	
mRNA degradation	$M_1 \rightarrow \varnothing$	1.3	
Protein degradation	$S_1 \rightarrow \varnothing$	1	
RNAP binding to DNA promoter	$D_2+P \rightleftharpoons D_2P$	10	500
Transcription	$D_2P \rightarrow D_2P+M_2$	5	
Translation	$M_2 \rightarrow M_2+S_2$	10	
mRNA degradation	$M_2 \rightarrow \varnothing$	1.3	
Protein degradation	$S_2 \rightarrow \varnothing$	1	
RNAP binding to DNA promoter	$D_0+P \rightleftharpoons D_0P$	10	960
S_1 binding to D_0P complex	$D_0P+S_1 \rightleftharpoons D_0PS_1$	10	500
S_2 binding to D_0P complex	$D_0P+S_2 \rightleftharpoons D_0PS_2$	10	500
S_2 binding to D_0PS_1 complex	$D_0PS_1+S_2 \rightleftharpoons D_0PS_1S_2$	10	250
S_1 binding to D_0PS_2 complex	$D_0PS_2+S_1 \rightleftharpoons D_0PS_1S_2$	10	250
Transcription	$D_0P \rightarrow D_0P+M_0$	0	
Transcription	$D_0S_1P \rightarrow D_0S_1P+M_0$	20	
Transcription	$D_0S_2P \rightarrow D_0S_2P+M_0$	20	
Transcription	$D_0PS_1S_2 \rightarrow D_0PS_1S_2+M_0$	20	
Translation	$M_0 \rightarrow M_0+S_0$	10	
mRNA degradation	$M_0 \rightarrow \varnothing$	1.3	
Protein degradation	$S_0 \rightarrow \varnothing$	1	

called extrinsic noise) [26], such as fluctuations in the number of RNA polymerase molecules or ribosomes, and variations in cell sizes. To explore the effect of extrinsic noise in more natural setting, we explicitly include the detailed processes, such as the DNA-binding proteins to recruit RNA polymerase and DNA state, in an extended set of chemical reactions (see Table II).

We perform realistic stochastic simulations of the whole circuit by using biologically reasonable parameter values and obtain three time series data of input TFs $S_1(t)$ and $S_2(t)$ and the output $S_0(t)$, according to the Gillespie algorithm [27]. We expect these simulations to faithfully reflect the biological system because the phage-λ is a well-studied system for which many parameters are measured and comparable models are capable of accurately reproducing distributions of protein concentrations in prokaryotic systems [28,29]. First, for two signals $X_1(t)$ and $X_2(t)$, we define the two-point dynamic correlation as

$$R_{x_1,x_2}(\tau)=\begin{cases}\dfrac{1}{N-|\tau|}\displaystyle\sum_{n=1}^{N-|\tau|}\tilde{x}_1(n)\tilde{x}_2(n+\tau), & \tau\geq 0\\ R_{x_2,x_1}(-\tau), & \tau<0,\end{cases} \tag{1}$$

where $\tilde{x}_i=X_i-\frac{1}{N}\Sigma_{n=1}^{N}X_i(n)$ with N being the number of point series. Then, we can similarly define the three-point dynamic cross-correlation function $R_{s_1s_2,s_0}(\tau)$ if we let $X_1=S_1S_2$ and $X_2=S_0$, and the four-point dynamic cross-correlation function $R_{s_1s_2,s_1s_2}(\tau)$ if we let $X_1=S_1S_2$ and $X_2=S_1S_2$. The three-point correlation function is normalized to

$$R(\tau)=\frac{R_{s_1s_1,s_0}(\tau)}{\sqrt{R_{s_1s_2,s_1s_2}(0)}\sqrt{R_{s_0,s_0}(0)}}. \tag{2}$$

Figure 2 shows the dependence of the normalized dynamic cross-correlation function $R(\tau)$ on the correlation time τ. Apparently, the correlation curve near the peak point close to the zero correlation time is upward convex for AND operation and downward convex for OR operation, whichever the sources of noise (intrinsic or extrinsic noise).

III. THEORETICAL ANALYSIS

The anticorrelation relationship between the convexity of dynamic cross-correlation functions for AND and OR operations as shown in the above section is not a casual finding but is a general fact. In what follows, we will analytically verify this point using a simple yet general model as schematized in Fig. 1.

A. Mathematical model

For the system described in Fig. 1, the corresponding biochemical process is modeled with the production and degra-

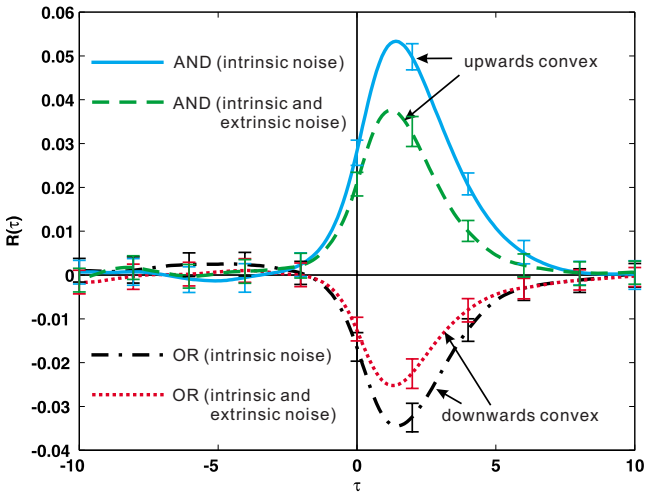

FIG. 2. (Color online) Geometric characteristics of dynamic cross correlations for the phage-λ operon, where 10^3 cells are measured and error bars described by the standard variance are shown. There is an anticorrelation relationship between the convexity of dynamic cross-correlation curves for AND and OR operations.

dation of the transcription factors and the output only

$$\emptyset \xrightarrow{\alpha_1} S_1 \xrightarrow{\beta_1} \emptyset,$$

$$\emptyset \xrightarrow{\alpha_2} S_2 \xrightarrow{\beta_2} \emptyset,$$

$$\emptyset \xrightarrow{\mathrm{CRIF}(S_1,S_2)} S_0 \xrightarrow{\beta_0} \emptyset, \tag{3}$$

where S_1 and S_2 represent the TF inputs to *cis*-regulatory module, S_0 is the measured output of the regulated gene, and arrows from and to $\emptyset$ denote synthesis and degradation, respectively. The production rate of S_0 is determined by the concentrations of the TFs and is encoded in the (dimensionless) $\mathrm{CRIF}(S_1,S_2)$.

When modeling the motion of individual species, we adapt the following standard Langevin equations:

$$\frac{dS_1}{dt} = \alpha_1 + E + I_1 - \beta_1 S_1,$$

$$\frac{dS_2}{dt} = \alpha_2 + E + I_2 - \beta_2 S_2,$$

$$\frac{dS_0}{dt} = E + I_0 - \beta_0 S_0 + \mathrm{CRIF}(S_1,S_2). \tag{4}$$

These equations include terms for protein production rate $(\alpha_i, i=1,2)$, protein degradation and dilution rate $(\beta_i, i=0,1,2)$, and the contributions of intrinsic and extrinsic noise sources (I_i, $i=0,1,2$ and E, respectively). Here, the extrinsic noise E is defined as a stochastic fluctuation to globally measured components, whereas the intrinsic noise is assumed as stochastic fluctuations in the gene expressions. Noise sources are modeled using Ornstein-Uhlenbeck processes by

$$\frac{dE}{dt} = -\beta_E E + \sigma_E \eta_E,$$

$$\frac{dI_i}{dt} = -\kappa_i I_i + \sigma_i \eta_i. \tag{5}$$

Assume that the white-noise terms η_E, η_1, η_2 and η_0 are independent, identically distributed processes with the zero mean and the unit standard deviation. The parameters β and κ define the time scale of the noise, while σ_E and σ_i set the standard deviation.

B. Analytic expressions of dynamic correlation functions

Denote $S_i^{eq} = \frac{\alpha_i}{\beta_i}$, $i=1,2$. We expect perturbations due to noise to be so small that it might be valid to approximate our system using the second-order Taylor expansion of CRIF at the origin. Define $s_i = S_i - S_i^{eq}$ $(i=0,1,2)$, where $S_0^{eq} = \mathrm{CRIF}(S_1^{eq}, S_2^{eq}) + a_0$ with $a_0 = \frac{g_{11}}{2}\langle\langle s_1^2\rangle\rangle_t + g_{12}\langle\langle s_1 s_2\rangle\rangle_t + \frac{g_{22}}{2}\langle\langle s_2^2\rangle\rangle_t$ in which the outside bracket represents the average over the time t, and g_{11}, g_{12}, g_{22} are two-order derivatives of the function CRIF with respect to variables S_1 and S_2 evaluated at the point (S_1^{eq}, S_2^{eq}). This will result in the following equations:

$$\frac{ds_1}{dt} = E + I_1 - \beta_1 s_1,$$

$$\frac{ds_2}{dt} = E + I_2 - \beta_2 s_2,$$

$$\frac{ds_0}{dt} = E + I_0 - \beta_0 s_0 + g_1 s_1 + g_2 s_2 + \frac{g_{11}}{2} s_1^2 + g_{12} s_1 s_2 + \frac{g_{22}}{2} s_2^2 - a_0. \tag{6}$$

For simplicity, we let $\beta = \beta_i$ and $\kappa = \kappa_i$ $(0 \le i \le 2)$, and additionally, assume $\beta \neq \kappa$, $\beta \neq 2\kappa$. By calculation, we find $a_0 = \frac{(g_{11}+2g_{12}+g_{11})\sigma_E^2}{8\beta^3} + \frac{g_{11}\sigma_1^2 + g_{22}\sigma_2^2}{4\beta\kappa(\beta+\kappa)}$ (see the Appendix). In addition, define the dynamic cross correlation between $s_0(t)$ and $s_1(t)/s_2(t)$ as

$$R_{s_1 s_2, s_0}(\tau) = \langle\langle s_1(t) s_2(t) s_0(t+\tau)\rangle\rangle_t, \tag{7}$$

where τ represents the correlation time. In simulations, this function is normalized to

$$R(\tau) = \frac{R_{s_1 s_1, s_0}(\tau)}{\sqrt{R_{s_1 s_2, s_1 s_2}(0)}\sqrt{R_{s_0, s_0}(0)}}. \tag{8}$$

In the presence of intrinsic noise only, by complex calculations we obtain the analytic expression of the dynamic cross-correlation function (also see the Appendix) denoted by $R_{in}(\tau)$

$$R_{in}(\tau) = \frac{g_{12}\sigma_1^2\sigma_2^2}{4\kappa^2(\beta^2-\kappa^2)^2}\begin{cases} \gamma e^{-\beta\tau} - \dfrac{\kappa^2}{\beta^3}e^{-2\beta\tau} + \dfrac{1}{\beta-2\kappa}e^{-2\kappa\tau} + \dfrac{2}{\beta}e^{-(\beta+\kappa)\tau}, & \tau \geq 0 \\ \dfrac{\kappa^2}{3\beta^3}e^{2\beta\tau} + \dfrac{1}{\beta+2\kappa}e^{2\kappa\tau} - \dfrac{2\kappa}{\beta(2\beta+\kappa)}e^{(\beta+\kappa)\tau}, & \tau < 0, \end{cases} \tag{9}$$

where $\gamma = -\frac{4(\beta+\kappa)(\beta-\kappa)^2(3\beta^2+12\kappa\beta+4\kappa^2)}{3\beta^3(\beta^2-4\kappa^2)(2\beta+\kappa)}$ is a constant depending on both β and κ. Note that the sign of g_{12} is opposite for the AND and OR operations (refer to Fig. 3). The simple analysis shows that $R_{in}(\tau)$ has one peak at some small $\tau_m > 0$. In addition, the convexity of $R_{in}(\tau)$ at a small interval of $\tau_m > 0$ but close to $\tau = 0$ is also anticorrelative for the two logic operations.

In the simultaneous presence of extrinsic and intrinsic noises, the total un-normalized cross-correlation function can be expressed in the form of

$$R_{s_1 s_2, s_0}(\tau) = R_{in}(\tau) + R_{ex}(\tau) + R_{mix}(\tau), \tag{10}$$

where the expression of $R_{in}(\tau)$ is given in Eq. (9), and

$$R_{ex}(\tau) = \frac{g_{11}+2g_{12}+g_{22}}{16\beta^7}\sigma_E^4\begin{cases} \left[\dfrac{152}{27}e^{-\beta\tau} - (5+4\beta\tau+\beta^2\tau^2)e^{-2\beta\tau}\right], & \tau \geq 0 \\ \dfrac{17-24\beta\tau+9\beta^2\tau^2}{27}e^{2\beta\tau}, & \tau < 0, \end{cases} \tag{11}$$

$$R_{mix}(\tau) = a_2\begin{cases} \left\{\left[\dfrac{3\beta+\kappa}{(2\beta+\kappa)^2} + \dfrac{\beta+\kappa}{\kappa^2} - \dfrac{22\kappa}{9\beta^2}\right]e^{-\beta\tau} + \dfrac{\kappa(2+\beta\tau)}{\beta^2}e^{-2\beta\tau} - \dfrac{\beta+\kappa(1+\beta\tau)}{\kappa^2}e^{-(\beta+\kappa)\tau}\right\}, & \tau \geq 0 \\ -\dfrac{\kappa(4-3\beta\tau)}{9\beta^2}e^{2\beta\tau} + \dfrac{3\beta+\kappa}{(2\beta+\kappa)^2}e^{(\beta+\kappa)\tau}, & \tau < 0, \end{cases} \tag{12}$$

with $a_2 = \frac{[(g_{11}+g_{12})\sigma_1^2+(g_{12}+g_{22})\sigma_2^2]\sigma_E^2}{8\kappa(\beta^2-\kappa^2)\beta^3}$. The derivation of all the above analytic expressions is put in the Appendix. Under some conditions (e.g., in the active region of transcription factors, see the numerical results in the next subsection), the dynamic cross-correlation function $R_{s_1 s_2, s_0}(\tau)$ has one peak at some small $\tau_m > 0$. In addition, the convexity of $R_{s_1 s_2, s_0}(\tau)$ at a small interval of $\tau_m > 0$ but close to $\tau = 0$ is also anticorrelative for the two logic operations. In particular, the convexity of $R_{ex}(\tau)$ has the anticorrelation for AND and OR gates in the presence of the extrinsic noise only.

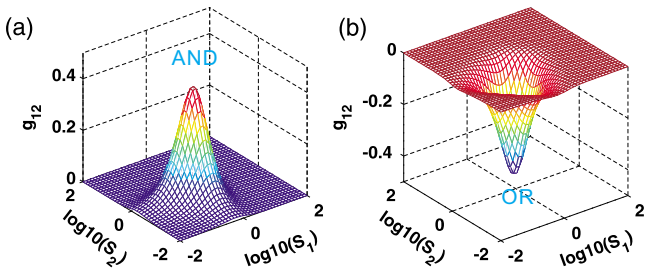

FIG. 3. (Color online) The second-order mixed-partial derivatives (g_{12}) with respect to S_1 and S_2. Parameter values are $\alpha_0 = 1$, $n = 2$, and $K = K_1 = K_2 = 100$.

To that end, we have analytically verified that the three-point dynamic cross-correlation function is upward convex for the AND operation, whereas downward convex for the OR operation, whichever sources of noise (intrinsic or extrinsic and both). Numerical simulation will further verify it (see the subsection for details).

C. Numerical results

If the binding and unbinding of transcription factors to the DNA sites are taken to be fast, CRIF [1,5,24,30–34] can be set as

$$\mathrm{CRIF}(S_1, S_2) = \alpha_0 \frac{r_0 + r_1(S_1/K_1)^n + r_2(S_2/K_2)^n + r_{12}(S_1/K_1)^n(S_2/K_2)^n}{1 + (S_1/K_1)^n + (S_2/K_2)^n + (S_1/K_1)^n(S_2/K_2)^n}, \tag{13}$$

where α_0 describes the dimensionless transcription rate, $K_i (i = 1, 2)$ is the (equilibrium) dissociation constant for the binding of the transcription factor $S_1 (i = 1, 2)$, and n is the Hill coefficient, which describes the cooperativity. For AND gate, both regulators must be bound to initiate transcription so $r_0 = r_1 = r_2 = 0$ and $r_{12} = 1$, whereas for OR gate, binding of

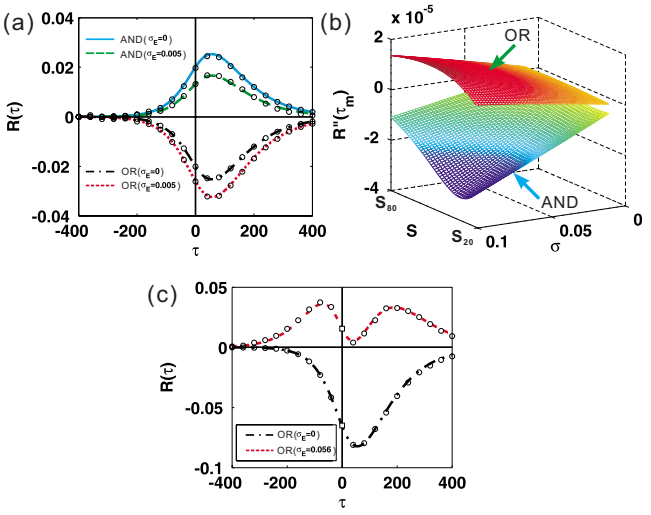

FIG. 4. (Color online) Description of dynamic cross correlations in the modeled system. (a) The geometric characteristic of the normalized correlation function $R(\tau)$, where $K=100$ nM, $\kappa=0.02/\text{min}$, $n=2$, $\beta=0.01/\text{min}$, $\alpha_0=4$, $\alpha_1=1$ mol/cell/min, $\alpha_2=1$ mol/cell/min, and $\sigma_0=\sigma_1=\sigma_2=0.02$. The empty circles represent simulated results, whereas the symbols indicated in the figure represent theoretical results; (b) the dependence of the two-order derivative of the correlation function evaluated at the peak point denoted by $R''(\tau_m)$ on the noise intensity σ, where $\sigma=\sigma_0=\sigma_1=\sigma_2$, $\sigma_E=\sigma/20$, $S=S_1=S_2$, and the other parameters are similar to those in (a). S_{20} and S_{80} represent 20% and 80% maximal values of the input signal concentrations, respectively. (c) An example that in the case of OR gate, the extrinsic noise can shift the dynamic cross-correlation curve upward such that the value of $R(\tau)$ at the zero correlation time $R(0)$ may be more than zero, where some of parameter values are slightly modified in contrast to those in (a) or (c).

either regulator enables the maximal production so that $r_0=0$ and $r_1=r_2=r_{12}=1$.The mixed-partial derivative is

$$g_{12} \triangleq \frac{\partial \text{CRIF}(S_1,S_2)}{\partial S_1\,\partial S_2} = \frac{(r_0+r_{12}-r_1-r_2)\alpha_0 n^2 (S_1/K_1)^n (S_2/K_2)^n}{S_1 S_2[1+(S_1/K_1)^n]^2[1+(S_2/K_2)^n]^2}. \quad (14)$$

Figure 3 shows the dependence of the second-order mixed-partial derivatives (g_{12}) on the input signal concentrations. This figure can help us find the active region.

Figure 4(a) shows that the extrinsic noise does not influence the convexity of the correlation function $R(\tau)$ for both logic operations, where the theoretical results are in good accord with the numerical results. Furthermore, Fig. 4(b) shows that the convexity of $R(\tau)$ is robust to noise in the active region of the two input signals (here, for the active region we mean that concentrations of the input signals are beyond 20% of their maximal values [25]) since the two-order derivative of $R(\tau)$ evaluated at the peak point, the sign of which describes the local convexity of $R(\tau)$, is always negative (i.e., upward convex) for the AND operation, whereas positive (i.e., downward convex) for the OR operation. Figure 4(c) shows an example that in the case of OR gate, the extrinsic noise can shift the dynamic cross-correlation curve upward such that the value of $R(\tau)$ at the zero correlation time $R(0)$ may be more than zero. The combination of Fig. 4(a) and 4(c) indicates that the static cross correlation (i.e., the cross correlation at the zero correlation time) does not have anticorrelation for AND and OR operations, but the convexity of the dynamic cross-correlation curves still has anticorrelation. In this case, Warmflash and Dinner's approach of detecting modes of combinatorial regulation is invalid. These results indicate that dynamic cross correlations can have more advantages than static cross correlations for signatures of combinatorial regulation in gene expression noise.

IV. CONCLUSION AND DISCUSSIONS

We have shown that the dynamic cross-correlation functions for AND and OR operations in gene expression noise have apparently distinct geometric characteristics (convexity). Such a difference is qualitative, depending neither on specific models nor on the sources of noise and, hence, the essential difference reflected by the modes of combinatorial regulation. More importantly, since the dynamic correlation function utilizes statistics of the naturally arising fluctuations in the copy number of the species, its geometric characteristics can in turn help us efficiently detect signatures of combinatorial regulation with available experimental data. This is useful because proximity in DNA binding is not sufficient to infer combinatorial interactions, and they cannot be readily probed by traditional methods (e.g., knockouts) or high-throughput expression assays (e.g., microarray data). Since stochastic fluctuations or noise exist inherently in biochemical reactions, using noise rather than external interference means to mine bioinformation related to gene regulation would provide a new research line. Regarding this aspect, there have been some works, e.g., Cox *et al.* used noise to characterize some genetic circuits [35], Dunlop *et al.* used correlation in gene expression noise to reveal the activity states of regulatory links [17], and Warmflash and Dinner used static cross correlations to detect signatures of combinatorial regulation in intrinsic biological noise [15]. We utilized dynamic cross correlations based on the nature of noise correlation to identify the modes of combinatorial regulation in intrinsic or extrinsic noise or both. In contrast to Warmflash and Dinner's approach, our approach would have some advantages since dynamic cross correlations can in general provide more information about gene-gene correlation in expression than static cross correlations, as shown above.

The method of dynamic cross correlation can also be extended to other situations of logic operations (ANDN, ORN, NAND, and NOR). For example, consider a system with two input TFs and the output of a gene. If both TFs are activators, this case has been studied in this paper; if both are repressors, our method can still show that the dynamic correlation function $R(\tau)$ is upward convex for NOR, whereas downward convex for NAND; if one TF is activator and the other is repressor, the $R(\tau)$ is upward convex for ANDN, whereas downward convex for ORN. In the cases of XOR and EQU, however, the approach will be invalid since the input TFs may be activator or repressor. Finally, the approach of dy-

namic cross correlation can be applied to other biological networks, e.g., RNA logic devices [36], nucleic acid logic circuits [37], signaling protein logic modules [38], to identify the types of logic operations.

Except for inferring synergies between regulators, the idea of dynamic correlation (e.g., two-point dynamic cross correlations introduced in Refs. [17,39]) can even be used to determine the direction and relationship of interactions between arbitrary two regulators, i.e., to determine who regulates whom and who activates/represses whom. In fact, we have shown that there is a time lag (τ_m) between the values of the dynamic cross-correlation function at the extreme point and the zero of the correlation time. Since the input regulator S_1 or S_2 actively regulates the expression of a target gene, we have $\tau_m > 0$. Practically, we can also calculate the time-correlation lag for arbitrarily two regulators. For example, we denote by A and B two regulators and assume that A acts on B without considering autoregulation. We compute the cross-correlation function between them with the time lag τ_m. If $\tau_m > 0$, this implies that A enhances B whereas if $\tau_m < 0$, this implies that A represses B. Apparently, such an inference approach can be extended to the case of arbitrarily many regulators and, thus, can infer the direction of interactions among them.

APPENDIX: THE DERIVATION OF DYNAMIC CROSS-CORRELATION FUNCTIONS

The purpose of this appendix is to derive all the analytic expressions given in the main text. From Eq. (6), we have

$$s_i(t) = s_i(0)e^{-\beta t} + \int_0^t e^{-\beta(t-t_1)}E(t_1)dt_1 + \int_0^t e^{-\beta(t-t_1)}I_i(t_1)dt_1,$$

$$i = 1,2,$$

$$\begin{aligned} s_0(t) = {} & s_0(0)e^{-\beta t} - a_0\int_0^t e^{-\beta(t-t_1)}dt_1 + \int_0^t e^{-\beta(t-t_1)}E(t_1)dt_1 \\ & + \int_0^t e^{-\beta(t-t_1)}I_0(t_1)dt_1 + g_1\int_0^t e^{-\beta(t-t_1)}s_1(t_1)dt_1 \\ & + g_2\int_0^t e^{-\beta(t-t_1)}s_2(t_1)dt_1 + \frac{g_{11}}{2}\int_0^t e^{-\beta(t-t_1)}s_1^2(t_1)dt_1 \\ & + g_{12}\int_0^t e^{-\beta(t-t_1)}s_1(t_1)s_2(t_1)dt_1 \\ & + \frac{g_{22}}{2}\int_0^t e^{-\beta(t-t_1)}s_2^2(t_1)dt_1. \end{aligned}$$

Our assumptions to noise imply

$$\begin{aligned} R_{s_1s_2,s_0}(\tau) \triangleq \langle\langle s_1(t)s_2(t)s_0(t+\tau)\rangle\rangle_t = {} & \left\langle\left\langle s_1(t)s_2(t)\left[-\frac{a_0}{\beta} + \frac{g_{11}}{2}\int_0^{t+\tau} e^{-\beta(t+\tau-t_1)}s_1^2(t_1)dt_1 + g_{12}\int_0^{t+\tau} e^{-\beta(t+\tau-t_1)}s_1(t_1)s_2(t_1)dt_1\right.\right.\right. \\ & \left.\left.\left. + \frac{g_{22}}{2}\int_0^{t+\tau} e^{-\beta(t+\tau-t_1)}s_2^2(t_1)dt_1\right]\right\rangle\right\rangle_t \\ = {} & \lim_{t\to\infty}\left\{-\frac{a_0}{\beta}\langle s_1(t)s_2(t)\rangle + e^{-\beta(t+\tau)}\int_0^{t+\tau} e^{\beta t_1}\left[\frac{g_{11}}{2}\langle s_1(t)s_2(t)s_1^2(t_1)\rangle + g_{12}\langle s_1(t)s_2(t)s_1(t_1)s_2(t_1)\rangle + \frac{g_{22}}{2}\langle s_1(t)s_2(t)s_2^2(t_1)\rangle\right]dt_1\right\}. \end{aligned}$$

Since the cross correlation defined above does not depend on initial conditions, we may set $s_i(0)=0$, $i=0,1,2$ (in other words, the initial values do not affect the resulting value of the dynamic cross correlation). Thus, we can express the cross correlation as

$$R_{s_1s_2,s_0}(\tau) = \lim_{t\to\infty} e^{-\beta(t+\tau)}\int_0^{t+\tau} e^{\beta t_1}\sum_{j=1}^{6} A_j(t_1)dt_1 - a, \quad \text{(A1)}$$

where

$$\begin{aligned} a = \frac{a_0}{\beta}\lim_{t\to\infty}\langle s_1(t)s_2(t)\rangle = {} & \frac{a_0}{\beta}\lim_{t\to\infty} e^{-2\beta t}\int_0^t\int_0^t e^{\beta(t_1+t_2)} \\ & \times\langle E(t_1)E(t_2)\rangle dt_1dt_2, \end{aligned}$$

$$\begin{aligned} a_0 = {} & \frac{g_{11}+2g_{12}+g_{22}}{2}\lim_{t\to\infty} e^{-2\beta t}\int_0^t\int_0^t e^{\beta(t_1+t_2)}\langle E(t_1)E(t_2)\rangle dt_1dt_2 \\ & + \frac{1}{2}\lim_{t\to\infty} e^{-2\beta t}\int_0^t\int_0^t e^{\beta(t_1+t_2)}[g_{11}\langle I_1(t_1)I_1(t_2)\rangle \\ & + g_{22}\langle I_2(t_1)I_2(t_2)\rangle]dt_1dt_2, \end{aligned}$$

$$\begin{aligned} A_1(t_1) = {} & \frac{g_{11}+2g_{12}+g_{22}}{2}e^{-2\beta(t+t_1)}\int_0^t\int_0^t\int_0^{t_1}\int_0^{t_1} e^{\beta(t_2+t_3+t_4+t_5)} \\ & \times\langle E(t_2)E(t_3)E(t_4)E(t_5)\rangle dt_2dt_3dt_4dt_5, \end{aligned}$$

$$A_2(t_1) = (g_{11} + g_{12})e^{-2\beta(t+t_1)} \int_0^t \int_0^t \int_0^{t_1} \int_0^{t_1} e^{\beta(t_2+t_3+t_4+t_5)} \times \langle E(t_2)E(t_4)I_1(t_3)I_1(t_5)\rangle dt_2 dt_3 dt_4 dt_5,$$

$$A_3(t_1) = (g_{12} + g_{22})e^{-2\beta(t+t_1)} \int_0^t \int_0^t \int_0^{t_1} \int_0^{t_1} e^{\beta(t_2+t_3+t_4+t_5)} \times \langle E(t_2)E(t_4)I_2(t_3)I_2(t_5)\rangle dt_2 dt_3 dt_4 dt_5,$$

$$A_4(t_1) = \frac{g_{11}}{2} e^{-2\beta(t+t_1)} \int_0^t \int_0^t \int_0^{t_1} \int_0^{t_1} e^{\beta(t_2+t_3+t_4+t_5)} \times \langle E(t_2)E(t_3)I_1(t_4)I_1(t_5)\rangle dt_2 dt_3 dt_4 dt_5,$$

$$A_5(t_1) = \frac{g_{22}}{2} e^{-2\beta(t+t_1)} \int_0^t \int_0^t \int_0^{t_1} \int_0^{t_1} e^{\beta(t_2+t_3+t_4+t_5)} \times \langle E(t_2)E(t_3)I_2(t_4)I_2(t_5)\rangle dt_2 dt_3 dt_4 dt_5,$$

$$A_6(t_1) = g_{12} e^{-2\beta(t+t_1)} \int_0^t \int_0^t \int_0^{t_1} \int_0^{t_1} e^{\beta(t_2+t_3+t_4+t_5)} \times \langle I_1(t_2)I_1(t_4)I_2(t_3)I_2(t_5)\rangle dt_2 dt_3 dt_4 dt_5.$$

Note that calculating the higher-order average of the noise E can be concluded as calculating its two-order average, thus, yielding that

$$\begin{aligned}\langle E(t_2)E(t_3)E(t_4)E(t_5)\rangle &= \langle E(t_2)E(t_3)\rangle\langle E(t_4)E(t_5)\rangle \\ &+ \langle E(t_2)E(t_4)\rangle\langle E(t_3)E(t_5)\rangle \\ &+ \langle E(t_2)E(t_5)\rangle\langle E(t_3)E(t_4)\rangle \\ &= \frac{\sigma_E^4}{4\beta^2}[e^{-\beta(|t_2-t_3|+|t_4-t_5|)} + e^{-\beta(|t_2-t_4|+|t_3-t_5|)} \\ &+ e^{-\beta(|t_2-t_5|+|t_3-t_4|)}]. \end{aligned} \tag{A2}$$

In addition, using the assumptions to noise we can have

$$\langle E(\tau_1)E(\tau_2)\rangle = \frac{\sigma_E^2}{2\beta} e^{-\beta|\tau_1-\tau_2|}, \quad \langle I_i(\tau_1)I_i(\tau_2)\rangle = \frac{\sigma_i^2}{2\kappa} e^{-\kappa|\tau_1-\tau_2|}, \tag{A3}$$

$$\begin{aligned}\langle E(\tau_1)E(\tau_2)I_i(\tau_3)I_i(\tau_4)\rangle &= \langle E(\tau_1)E(\tau_2)\rangle\langle I_i(\tau_3)I_i(\tau_4)\rangle \\ &= \frac{\sigma_E^2}{2\beta} e^{-\beta|\tau_1-\tau_2|} + \frac{\sigma_i^2}{2\kappa} e^{-\kappa|\tau_3-\tau_4|}, \end{aligned} \tag{A4}$$

$$i = 1,2,$$

$$\begin{aligned}\langle I_1(t_2)I_1(t_4)I_2(t_3)I_2(t_5)\rangle &= \langle I_1(t_2)I_1(t_4)\rangle\langle I_2(t_3)I_2(t_5)\rangle \\ &= \frac{\sigma_1^2\sigma_2^2}{4\kappa^2} e^{-\kappa(|t_2-t_4|+|t_3-t_5|)}. \end{aligned} \tag{A5}$$

The substitution of Eqs. (A2)–(A5) into the expressions of A_1-A_6, a and a_0, and further into $R_{s_1 s_2, s_0}(\tau)$ yields

$$R_{s_1 s_2, s_0}(\tau) = \lim_{t\to\infty} e^{-\beta(t+\tau)} \int_0^{t+\tau} e^{\beta t_1}[B_1(t_1) + B_2(t_1) + B_3(t_1) + B_4(t_1)]dt_1 - a, \tag{A6}$$

where

$$B_1(t_1) = \frac{g_{11} + 2g_{12} + g_{22}}{8\beta^2} \sigma_E^4 [F_1(t,t)F_1(t_1,t_1) + 2F_2^2(t,t_1)], \tag{A7}$$

$$B_2(t_1) = \frac{(g_{11} + g_{12})\sigma_1^2 + (g_{12} + g_{22})\sigma_2^2}{4\beta\kappa} \sigma_E^2 F_2(t,t_1)F_4(t,t_1), \tag{A8}$$

$$B_3(t_1) = \frac{g_{11}\sigma_1^2 + g_{22}\sigma_2^2}{8\beta\kappa} \sigma_E^2 F_1(t,t)F_3(t_1,t_1), \tag{A9}$$

$$B_4(t_1) = \frac{g_{12}\sigma_1^2\sigma_2^2}{4\kappa^2} F_4^2(t,t_1), \tag{A10}$$

$$a = \frac{\sigma_E^2}{8\beta^2} \lim_{t\to\infty} \left[\frac{(g_{11} + 2g_{12} + g_{22})\sigma_E^2}{\beta} F_1^2(t,t) + \frac{g_{11}\sigma_1^2 + g_{22}\sigma_2^2}{k} F_1(t,t)F_3(t,t) \right], \tag{A11}$$

with

$$F_1(t,t) \triangleq e^{-2\beta t} \int_0^t \int_0^t e^{\beta(t_2+t_3-|t_2-t_3|)} dt_2 dt_3, \tag{A12}$$

$$F_2(t,t_1) \triangleq e^{-\beta(t+t_1)} \int_0^t \int_0^{t_1} e^{\beta(t_2+t_3-|t_2-t_3|)} dt_2 dt_3, \tag{A13}$$

$$F_3(t,t) \triangleq e^{-2\beta t} \int_0^t \int_0^t e^{\beta(t_2+t_3)-\kappa|t_2-t_3|} dt_2 dt_3, \tag{A14}$$

$$F_4(t,t_1) \triangleq e^{-\beta(t+t_1)} \int_0^t \int_0^{t_1} e^{\beta(t_2+t_3)-\kappa|t_2-t_3|} dt_2 dt_3. \tag{A15}$$

By calculating these basic integrals, we can obtain the expressions of functions $B_i(t)$, that is,

$$B_1(t_1) \approx \frac{g_{11}+2g_{12}+g_{22}}{8\beta^2}\sigma_E^4 \begin{cases} \frac{1}{4\beta^4}+2\left[\frac{\beta(t-t_1)+1}{2\beta^2}\right]^2 e^{-2\beta(t-t_1)}, & 0 \le t_1 \le t \\ \frac{1}{4\beta^4}+2\left[\frac{\beta(t_1-t)+1}{2\beta^2}\right]^2 e^{-2\beta(t_1-t)}, & t_1 > t, \end{cases} \tag{A16}$$

$$B_2(t_1) \approx \frac{[(g_{11}+g_{12})\sigma_1^2+(g_{12}+g_{22})\sigma_2^2]\sigma_E^2}{4\beta\kappa} \begin{cases} \frac{1+\beta(t-t_1)}{2\beta^2(\beta^2-\kappa^2)}\left[-\frac{\kappa}{\beta}e^{-2\beta(t-t_1)}+e^{-(\beta+\kappa)(t-t_1)}\right], & 0 \le t_1 < t \\ \frac{1+\beta(t_1-t)}{2\beta^2(\beta^2-\kappa^2)}\left[-\frac{\kappa}{\beta}e^{-2\beta(t_1-t)}+e^{-(\beta+\kappa)(t_1-t)}\right], & t_1 > t, \end{cases} \tag{A17}$$

$$B_3(t_1) \approx \frac{(g_{11}\sigma_1^2+g_{22}\sigma_2^2)\sigma_E^2}{16\kappa(\beta+\kappa)\beta^4}, \tag{A18}$$

$$B_4(t_1) \approx \frac{g_{12}\sigma_1^2\sigma_2^2}{4\kappa^2(\beta^2-\kappa^2)^2} \begin{cases} \left[e^{-\kappa(t-t_1)}-\frac{\kappa}{\beta}e^{-\beta(t-t_1)}\right]^2, & 0 \le t_1 \le t \\ \left[e^{-\kappa(t_1-t)}-\frac{\kappa}{\beta}e^{-\beta(t_1-t)}\right]^2, & t_1 > t, \end{cases} \tag{A19}$$

$$a = \frac{(g_{11}+2g_{12}+g_{22})\sigma_E^4}{32\beta^7}+\frac{(g_{11}\sigma_1^2+g_{22}\sigma_2^2)\sigma_E^2}{16\kappa(\beta+\kappa)\beta^5}, \tag{A20}$$

where "≈" means that the resulting expressions do not influence the limit value in Eq. (A6). To that end, we can easily derive the expression of $R_{s_1 s_2, s_0}(\tau)$ in Eq. (A6), as shown in the main text. The normalization factor can be similarly derived.

[1] U. Alon, *An Introduction to Systems Biology: Design Principles of Biological Circuits* (Chapman & Hall, Boca Raton, FL, 2007).
[2] L. Glass and S. A. Kayffman, J. Theor. Biol. **39**, 103 (1973).
[3] A. Arkin and J. Ross, Biophys. J. **67**, 560 (1994).
[4] A. A. Margolin and M. N. Stojanovic, Nat. Biotechnol. **23**, 1374 (2005).
[5] A. E. Mayo *et al.*, PLoS Biol. **4**, e45 (2006).
[6] M. Carmona *et al.*, J. Bacteriol. **187**, 125 (2005).
[7] G. Bertoni, S. Marques, and V. de Lorenzo, Mol. Microbiol. **27**, 651 (1998).
[8] C. H. Yuh, H. Bolouri, and E. H. Davidson, Science **279**, 1896 (1998).
[9] J. J. Zhang, Z. J. Yuan, and T. S. Zhou, Phys. Rev. E **79**, 041903 (2009).
[10] M. B. Elowitz *et al.*, Science **297**, 1183 (2002).
[11] W. J. Blake *et al.*, Nature (London) **422**, 633 (2003).
[12] M. Kaern *et al.*, Nat. Rev. Genet. **6**, 451 (2005).
[13] T. S. Zhou, L. N. Chen, and K. Aihara, Phys. Rev. Lett. **95**, 178103 (2005).
[14] N. G. van Kapmen, *Stochastic Process in Physics and Chemistry* (North-Holland, Amsterdam, 1992).
[15] A. Warmflash and A. R. Dinner, Proc. Natl. Acad. Sci. U.S.A. **105**, 17262 (2008).
[16] A. Arkin, P. Shen, and J. Ross, Science **277**, 1275 (1997).
[17] M. J. Dunlop *et al.*, Nat. Genet. **40**, 1493 (2008).
[18] C. Creighton and S. Hanash, Bioinformatics **19**, 79 (2003).
[19] C. T. Chen, J. C. Wang, and B. A. Cohen, Am. J. Hum. Genet. **80**, 692 (2007).
[20] Y. Pilpel, P. Sudarsanam, and G. M. Church, Nat. Genet. **29**, 153 (2001).
[21] H. K. Tsai *et al.*, Proc. Natl. Acad. Sci. U.S.A. **102**, 13532 (2005).
[22] J. Gertz, E. D. Siggia, and B. A. Cohen, Nature (London) **457**, 215 (2009).
[23] J. K. Joung, D. M. Koepp, and D. Hochschild, Science **265**, 1863 (1994).
[24] Y. Setty *et al.*, Proc. Natl. Acad. Sci. U.S.A. **100**, 7702 (2003).
[25] F. J. Isaacs *et al.*, Proc. Natl. Acad. Sci. U.S.A. **100**, 7714 (2003).
[26] J. Hasty *et al.*, Proc. Natl. Acad. Sci. U.S.A. **97**, 2075 (2000).
[27] D. T. Gillespie, J. Comput. Phys. **22**, 403 (1976).
[28] N. J. Guido *et al.*, Nature (London) **439**, 856 (2006).
[29] J. T. Mettetal *et al.*, Proc. Natl. Acad. Sci. U.S.A. **103**, 7304 (2006).
[30] N. E. Buchler, U. Gerland, and T. Hwa, Proc. Natl. Acad. Sci. U.S.A. **100**, 5136 (2003).
[31] L. Bintu *et al.*, Curr. Opin. Genet. Dev. **15**, 116 (2005).
[32] R. Hermsen, S. Tans, and P. R. ten Wolde, PLOS Comput. Biol. **2**, e164 (2006).
[33] M. Gerstung, J. Timmer, and C. Fleck, Phys. Rev. E **79**, 011923 (2009).
[34] R. Silva-Rocha and V. de Lorenzo, FEBS Lett. **582**, 1237 (2008).
[35] C. D. Cox *et al.*, Proc. Natl. Acad. Sci. U.S.A. **105**, 10809 (2008).
[36] M. N. Win and C. D. Smolke, Science **322**, 456 (2008).
[37] G. Seelig *et al.*, Science **314**, 1585 (2006).
[38] K. E. Prehoda *et al.*, Science **290**, 801 (2000).
[39] G. Nolte *et al.*, Phys. Rev. Lett. **100**, 234101 (2008).